PERFORMANCE AND PREDICTION OF MARINE CLAY TREATED WITH VACUUM AND SURCHARGE CONSOLIDATION AT PORT OF BRISBANE

Buddhima Indraratna[1], A.S. Balasubramaniam[2], Harry Poulos[3], Cholachat Rujikiatkamjorn[4] and Jayantha Ameratunga[5]

[1]*Professor, Centre for Geomechanics and Railway Engineering, University of Wollongong, Wollongong, NSW 2522, (corresponding author). E-mail: indra@uow.edu.au*
[2]*Adjunct Professor, School of Civil Engineering Griffith University, Gold Coast, Queensland, Australia*
[3]*Senior Principal, Coffey Geotechnics, 8/12 Mars Road Lane Cove West NSW 2066 Australia*
[4]*Associate Professor, Centre for Geomechanics and Railway Engineering, University of Wollongong, Wollongong, NSW 2522, Australia.*
[5]*Senior Principal, Coffey Geotechnics, 47 Doggett Street Newstead QLD 4006 Australia*

ABSTRACT

During the past decade, the application of vacuum preloading for stabilising soft coastal clay and other low-lying estuarine soils has become popular in Australia. The cost-effectiveness is a major factor in most projects in view of the significantly reduced time for achieving a relatively high degree of consolidation. Due to an increase in trade activities at the Port of Brisbane, new facilities on Fisherman Islands at the mouth of the Brisbane River will be constructed on the new outer area (235 ha) adjacent to the existing port facilities via land reclamation. A vacuum assisted surcharge load and conventional surcharge scheme in conjunction with prefabricated vertical drains was selected to reduce the required consolidation time through the deeper subsoil layers. The performance of the combined vacuum and surcharge fill system and the construction of the embankment are described in this paper. A comparison of the performance of the vacuum combined surcharge loading system with a standard surcharge fill highlights the clear benefits of vacuum consolidation. Field monitoring data are presented to demonstrate how the embankment performed during construction. The paper also evaluates the relative performance of the two contrasting preloading systems (i.e. vacuum and non-vacuum system). An analytical solution for radial consolidation considering both time-dependent surcharge loading and vacuum pressure is proposed to predict the settlements and associated excess pore pressures of the soft Holocene clay deposits.

1 INTRODUCTION

Coastal regions of Australia contain soft clays, which have unacceptable geotechnical properties such as, low shear strength and high compressibility. In the absence of suitable ground improvement, excessive differential settlement and lateral movement unfavourably affect the stability of buildings and port infrastructure built on such soft ground (Holtz *et al*., 1991, Indraratna and Redana, 2000). A system of vertical drains with a combined vacuum and surcharge preloading is an effective method for promoting radial flow, which accelerates soil consolidation. The behaviour of soft clay stabilized with vertical drains and vacuum pressure can now be predicted with acceptable accuracy due to significant progress that has been made in the past decade through rigorous analytical and numerical analysis. Mohamedelhassan and Shang (2002) proposed an analytical solution for one-dimensional consolidation with vacuum application. Indraratna *et al*. (2005) extended the unit cell radial consolidation theory for vacuum application with instantaneous loading considering the vacuum loss along the drain length.

The Port of Brisbane is Australia's third largest container port located between the mouth of the Brisbane River and Fisherman Islands (Indraratna *et al*., 2011). With rapid growth in trading activities, a new outer area (235 ha) adjacent to the current port facilities is being reclaimed to maximise the available land, and to provide the additional berths suitable for cargo and container handling. In this area, the soil profile comprises a highly compressible clay layer over 30 m in thickness with an undrained shear strength of less than 15 kPa near the surface. The strength of the dredged mud used for reclamation has a much lower shear strength depending on the time of placement and the duration the capping material (surcharge) had been in place. Without surcharge preloading, it is determined that the consolidation will take more than 50 years with vertical settlements of 2.5-4.0 m expected under the required service loadings. Therefore, vacuum consolidation with prefabricated vertical drains (PVDs) was suggested to speed up the consolidation process and to limit horizontal deformation for the site located immediately adjacent to the Moreton Bay Marine Park (Austress Menard, 2008).

Chu *et al*. (2000) and Chai *et al.* (2005) discussed the application of the vacuum preloading combined with PVDs. In this method, the suction can propagate to a greater depth of the subsoil using the PVD system. Also, lengthy consolidation time due to stage construction can be minimized (Indraratna *et al.,* 2005, Sathananthan *et al*., 2008). The

surcharge fill height may be lowered by several metres, if a vacuum pressure of at least 70% the atmospheric pressure is sustained (Rujikiatkamjorn *et al*., 2008). In addition, the embankment construction rate can be increased with the reduction in the number of construction stages (Yan and Chu, 2003). Once the soil increases its stiffness and shear strength due to consolidation, the post-construction settlement can be considerably less, thereby reducing risk of differential settlement (Shang *et al*., 1998). The ground improvement provided by PVDs combined with vacuum pressure may be an economically attractive alternative in deep soft clay sites. To date, there is no comprehensively reported case history where both the conventional surcharge preloading and vacuum technique are applied in the same area with different drain types and spacing.

In this paper, the performance comparison between the vacuum and non-vacuum area has been made based on the measured vertical deformations, excess pore pressures and horizontal displacements. The effects of drain spacing, drain type and improvement technique are elaborated based on the observed degree of consolidation. The analytical solutions for radial consolidation considering both time dependent surcharge loading and vacuum pressure are proposed to predict settlement and associated excess pore pressure.

2 ANALYTICAL SOLUTIONS FOR VACUUM PRELOADING SYSTEMS

2.1 VACUUM PRELOADING SYSTEMS

Currently, there are two main types of vacuum preloading systems adopted in the field (Geng *et al*., 2012):

A. Membrane system: After PVDs are installed and the sand blanket is placed with horizontal perforated pipes, the membrane is laid on the top and its borders are submerged under a bentonite slurry trench (Figure 1a). The vacuum pumps are then attached to the discharge system. A major advantage of this system is that the vacuum can distribute within the sand platform, along the soil surface and down the PVDs. However, an obvious drawback is that the efficiency of the entire system depends on the ability of the airtight system to prevent any air leaks over a significant period of time.

B. Membraneless system: When an area has to be subdivided and progressed individually, the vacuum preloading can only be conducted one section after another and therefore the membrane system may not be an economical solution. To avoid this problem, the vacuum pipes are connected directly to each individual PVD using a tubing system (Figure 1b). In contrast to the membrane system where any air leak can affect the entire system, each drain acts independently. However, the requirement of significant tubing for hundreds of drains can affect the installation time and cost.

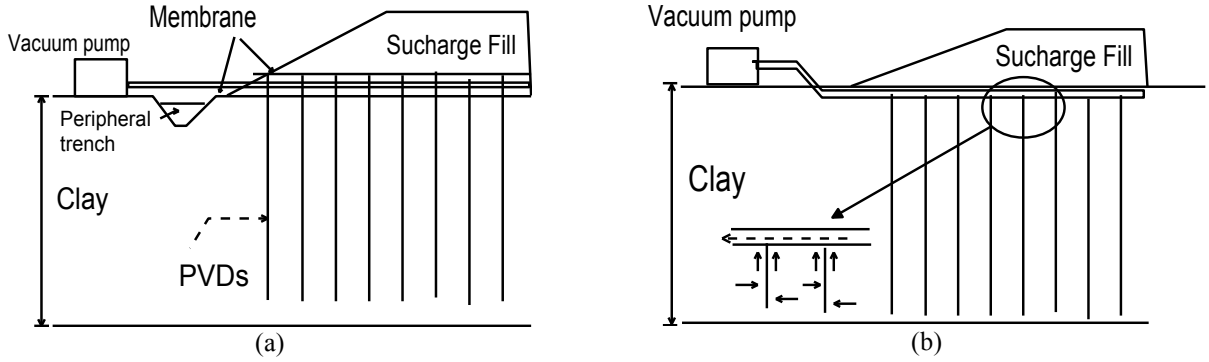

Figure 1: Types of vacuum preloading systems (a) Membrane system and (b) Membraneless system.

2.2 GOVERNING EQUATIONS

2.2.1 Membrane system

In a membrane system, the vacuum propagates from the horizontal drain through layer of sand, PVDs, and layer of clay (Figure 2a). This three dimensional flow in the sand blanket beneath the membrane ($0 \le z \le L_w$) can be expressed as:

$$\frac{\partial \varepsilon_{v1}}{\partial t} = -m_{v1}\left(\frac{\partial \bar{u}_1}{\partial t} - \frac{dq}{dt}\right) \tag{1}$$

$$-\frac{k_{h1}}{\gamma_w}\left(\frac{1}{r}\frac{\partial u_1}{\partial r} + \frac{\partial^2 u_1}{\partial r^2}\right) - \frac{k_{v1}}{\gamma_w}\frac{\partial^2 \bar{u}_1}{\partial z^2} = \frac{\partial \varepsilon_{v1}}{\partial t} \quad r_w \le r \le r_e \tag{2}$$

$$\frac{\partial^2 u_{w1}}{\partial z^2} = -\frac{2k_{h1}}{r_w k_{v1}} \frac{\partial u_1}{\partial r}\bigg|_{r=r_w} \tag{3}$$

$$\bar{u}_1 = \frac{1}{\pi(r_e^2 - r_w^2)} \int_{r_w}^{r_e} 2\pi r u_1 dr \tag{4}$$

The governing equations for the underlying soil ($L_w \le z \le H$), may be expressed as:

$$\frac{\partial \varepsilon_{v2}}{\partial t} = -m_{v2}\left(\frac{\partial \bar{u}_2}{\partial t} - \frac{dq}{dt}\right) \tag{5}$$

$$-\frac{k_{s2}}{\gamma_w}\left(\frac{1}{r}\frac{\partial u_{s2}}{\partial r} + \frac{\partial^2 u_{s2}}{\partial r^2}\right) - \frac{k_{v2}}{\gamma_w}\frac{\partial^2 \bar{u}_2}{\partial z^2} = \frac{\partial \varepsilon_{v2}}{\partial t} \qquad r_w \le r \le r_s \tag{6}$$

$$-\frac{k_{h2}}{\gamma_w}\left(\frac{1}{r}\frac{\partial u_{n2}}{\partial r} + \frac{\partial^2 u_{n2}}{\partial r^2}\right) - \frac{k_{v2}}{\gamma_w}\frac{\partial^2 \bar{u}_2}{\partial z^2} = \frac{\partial \varepsilon_{v2}}{\partial t} \qquad r_s \le r \le r_e \tag{7}$$

$$\frac{\partial^2 u_{w2}}{\partial z^2} = -\frac{2k_{s2}}{r_w k_w} \frac{\partial u_{s2}}{\partial r}\bigg|_{r=r_w} \tag{8}$$

$$\bar{u}_2 = \frac{1}{\pi(r_e^2 - r_w^2)}\left(\int_{r_w}^{r_s} 2\pi r u_{s2} dr + \int_{r_s}^{r_e} 2\pi r u_{n2} dr\right) \tag{9}$$

The boundary conditions for both the radial and vertical directions are as follows:

$$r = r_e: \frac{\partial u_{n2}}{\partial r} = 0, \frac{\partial u_1}{\partial r} = 0 \tag{10a}$$

$$r = r_s: k_{s2}\frac{\partial u_{s2}}{\partial r} = k_{h2}\frac{\partial u_{n2}}{\partial r} \tag{10b}$$

$$r = r_s: u_{s2} = u_{n2} \tag{10c}$$

$$r = r_w: u_{s2} = u_{w2}, \bar{u}_1 = u_{w1} \tag{10d}$$

$$z = 0: u_{w1} = p, \bar{u}_1 = p \tag{10e}$$

$$z = H: \frac{\partial u_{w2}}{\partial z} = 0, \frac{\partial \bar{u}_2}{\partial z} = 0 \tag{10f}$$

Continuity at the interface between the sand blanket and underlying layer of soil ($z = L_w$) may be then written as:

$$z = L_w: u_{w1} = u_{w2} \tag{10g}$$

$$z = L_w: \bar{u}_1 = \bar{u}_2 \tag{10h}$$

$$z = L_w: k_{v1}\frac{\partial u_{w1}}{\partial z} = k_w \frac{\partial u_{w2}}{\partial z} \tag{10i}$$

$$z = L_w: k_{v1}\frac{\partial \bar{u}_1}{\partial z} = k_{v2}\frac{\partial \bar{u}_2}{\partial z} \tag{10j}$$

The initial condition is:

$$\text{At } t = 0, \quad \bar{u}_1 = \bar{u}_2 = u_0(z) = q_0 \tag{10k}$$

where i is the index number of arbitrary layer, ($i = 1, 2$), r_{si} is the radius of smear zone, r_e is the radius of influence zone, r is the radial coordinate, z is the vertical coordinate, t is the time, ε_{vi} is the vertical strain, m_{vi} is the coefficient of volume compressibility of soil, k_{hi} is the horizontal coefficient of permeability of soil, k_{vi} is the vertical coefficient of permeability of the soil, k_w is the coefficient of permeability of the vertical drain, $\bar{u}_i$ is the average pore pressure, u_{si} is the pore pressure at any point in the smear zone, u_{ni} is the pore pressure at any point in the natural soil

zone, u_{wi} is the excess pore water pressure within the vertical drain, q is the time-dependent surcharge preloading, q_0 is the initial value of preloading, L_w is the thickness of the sand layer, H is the thickness of the whole layer (i.e., for the membrane system, (both sand blanket and clay layer and for the membraneless system, only the clay layer), p is the vacuum pressure.

2.2.2 Membraneless system

The main difference between a membrane system and a membraneless system are the boundary conditions. In the membraneless system a vacuum pump is connected directly to individual PVD's through a system of horizontal pipes (Figure 2b). The governing equations and initial conditions of underlying soil improved by PVD's are the same as for the membrane system (Eq. 10a)-Eq. 10d and Eq. 10k). In order to study the loss of vacuum, the vacuum pressure along the boundary of the drain was considered to vary linearly from p at the top of the drain to ηp at the bottom, where η is a ratio between the vacuum at the top and bottom of the drain. The value of η varies between 0 and 1. If there is no vacuum loss at the bottom of the PVDs η =1, and if vacuum pressure is 0 at the bottom of the drain, η = 0.

The boundary conditions for a membraneless system are:

$$z = 0: u_w = p, \frac{\partial \bar{u}}{\partial z} = 0 \tag{10m}$$

$$z = H: \frac{\partial u_w}{\partial z} = \frac{\eta - 1}{H} p, \frac{\partial \bar{u}}{\partial z} = 0 \tag{10n}$$

The analytical solutions based on the above governing equations and boundary conditions are given in Appendix 1 for both membrane and membraneless systems.

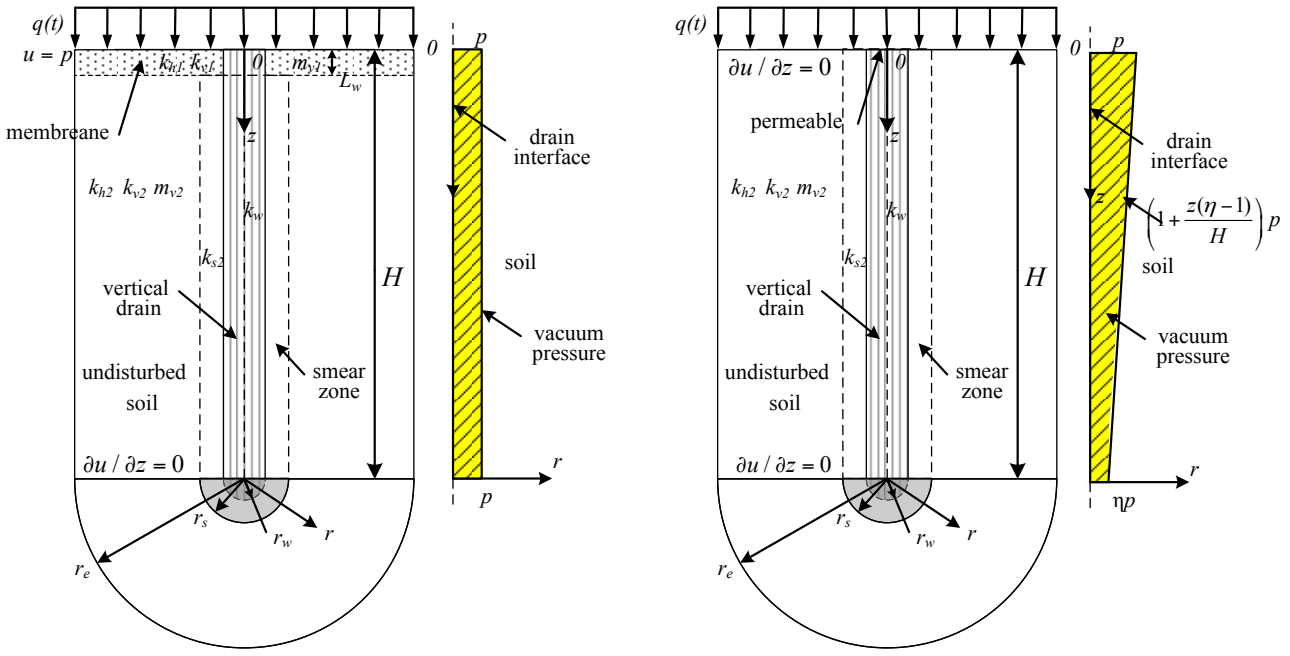

(a) (b)

Figure 2: Analysis schemes of unit cell with vertical drain: (a) membrane system and (b) membraneless system (Geng *et al*., 2012).

3 GENERAL DESCRIPTION OF EMBANKMENT CHARACTERISTICS AND SITE CONDITIONS

In 2003, the Port of Brisbane Corporation started to reclaim a sub-tidal land area of 235 ha at Fisherman Islands near the mouth of the Brisbane River (Figure 3). The reclaimed land is expected to provide additional berths and associated infrastructure to accommodate the future growth of the Port (Port of Brisbane Corporation, 2009). To compare the

performance of the vacuum system with the non-vacuum system (PVD and surcharge load), a trial area is shown in Figure 4. There were 3 contractors selected to carry out this trials. Each contractor was assigned an area of about 3 ha for the trial. The aim was to compare performance based on their design and construction work.

Contractor A had 8 trial areas in Area S3a, designated as WD1, WD2, WD3, WD4, WD5a, WD5b, VC 1 and VC 2. Areas WD1 to WD5a and WD5b had surcharge only, while VC1 and VC2 had surcharge and vacuum consolidation with membrane system.

Contractor B: Their trial area T11 consisted of seven areas. Five had surcharge and different drain types. Two had surcharge in conjunction with membraneless system.

Contractor C: Their trial area in T11 was subdivided into Areas 4, 5 and 6. Areas 4 and 5 had a surcharge period of a year, whereas Area 6 had a surcharge period of 0.5 years. Vertical drains with 1.4 m spacing were adopted in Areas 4 and 5 while Area 6 used vertical drains with a spacing of 1 m.

The upper Holocene sand underneath the dredged mud was about 2-3m thick, and overlaid the Holocene clay layer having a thickness from 6 m to 25 m. The highly compressible Holocene clay layer had a low shear strength and is generally referred to as PoB clay (Ameratunga *et al*., 2010). The Holocene layer overlies a Pleistocene deposit comprising of highly over-consolidated clay. Site investigations including cone penetration/piezocone tests, dissipation tests, boreholes, field vane shear tests and oedometer tests were carried out to assess the consolidation and stability design parameters. The soil profile and the corresponding soil properties are shown in Figure 5, where groundwater level is at +3.5m RL. The water contents of the soil layers were at or beyond their liquid limits. The field vane tests indicate that the undrained shear strength of the dredged mud and the Holocene clays varied from 5 kPa to 60 kPa. The compression index (C_c) varied from 0.1-1.0. The coefficient of consolidation in vertical direction (c_v) was approximately the same as that in horizontal direction (c_h) for the totally remoulded dredged mud layer, while c_v/c_h is about 2 for the Holocene clay layer.

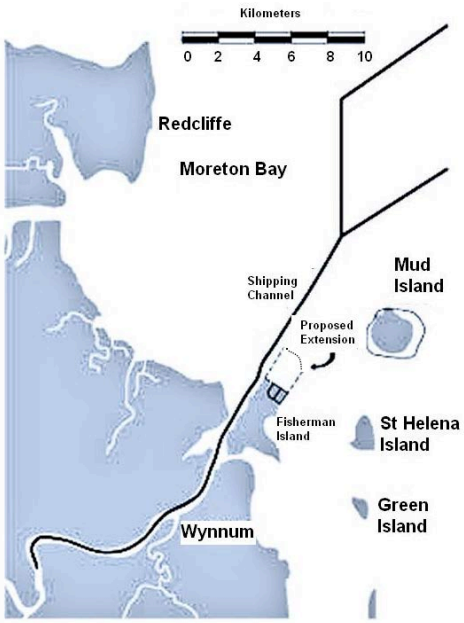

Figure 3. Map of the proposed extension area at the Port of Brisbane (adopted from Port of Brisbane Corporation, 2009)

As the Holocene clay layer is quite thick, two preloading approaches were used to minimise the long term settlement including conventional surcharge preloading system and the vacuum consolidation system both applied to PVDs. Rigorous design specifications were considered for the design and construction of fill embankments and vacuum application over the soft Holocene deposits: (a) Service load of 15-25 kPa, (b) maximum residual settlement of not more than 250 mm over 20 years after the application of service load.

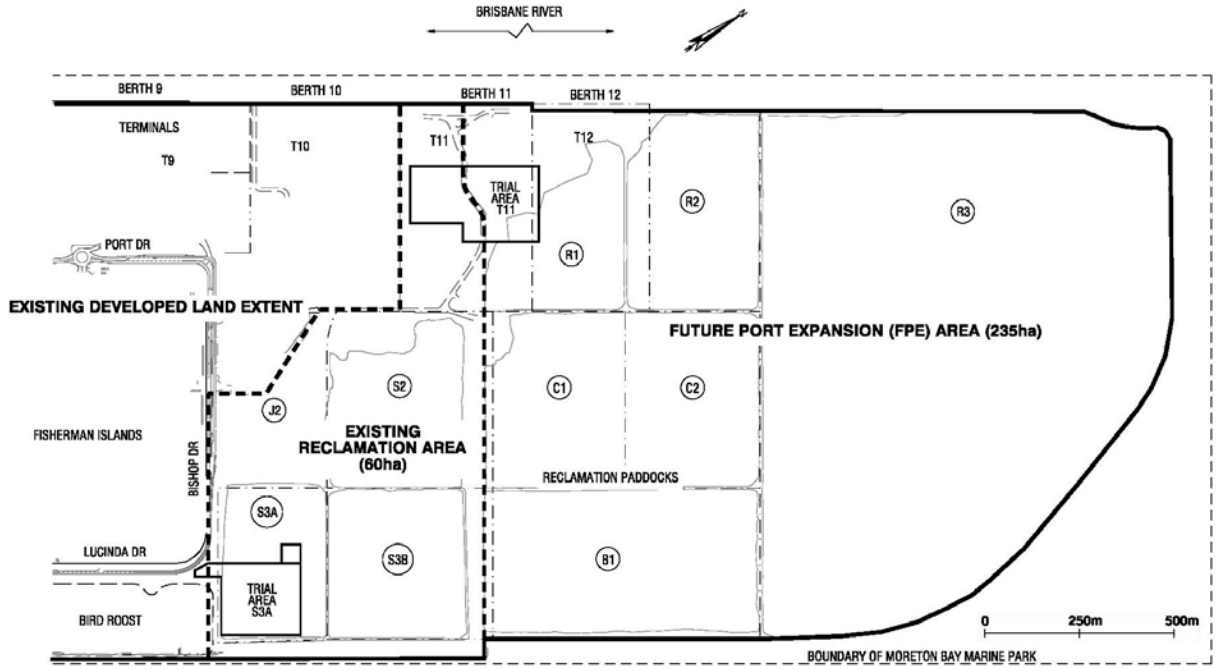

Figure 4: General site layout.

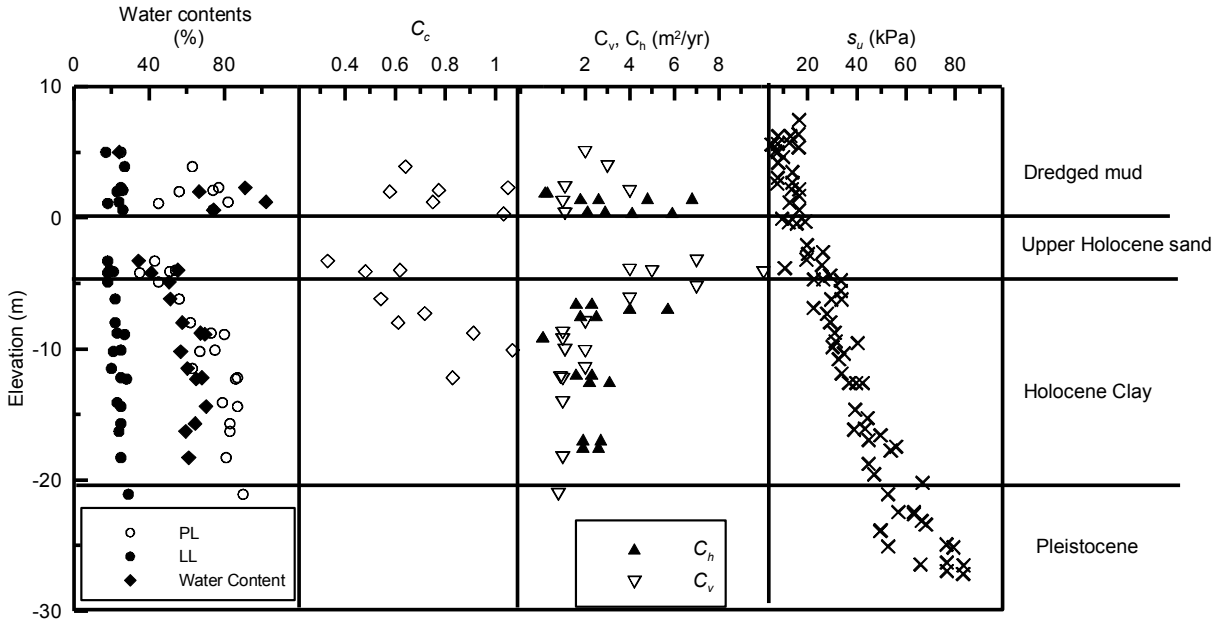

Figure 5: Soil properties and profile at S3A, Port of Brisbane (Indraratna *et al*., 2011).

4 ASSESSMENT OF RELATIVE EFFECTIVENESS OF THE TRIAL SCHEMES

4.1 DEGREE OF CONSOLIDATION WITH TIME

The numerically determined DOC with time plots is shown in Figure 6 for an array of locations, and they all show a very similar behaviour, irrespective of the treatment site (S3A and T11) and the type of improvement (vacuum vs. surcharge only). In all these settlement plate areas, a relatively high DOC has been achieved after one year, and all plots converge to DOC > 80%. In order to separate the 'clustering' especially towards one year, the DOC is divided by the dimensionless parameter *β-factor*.

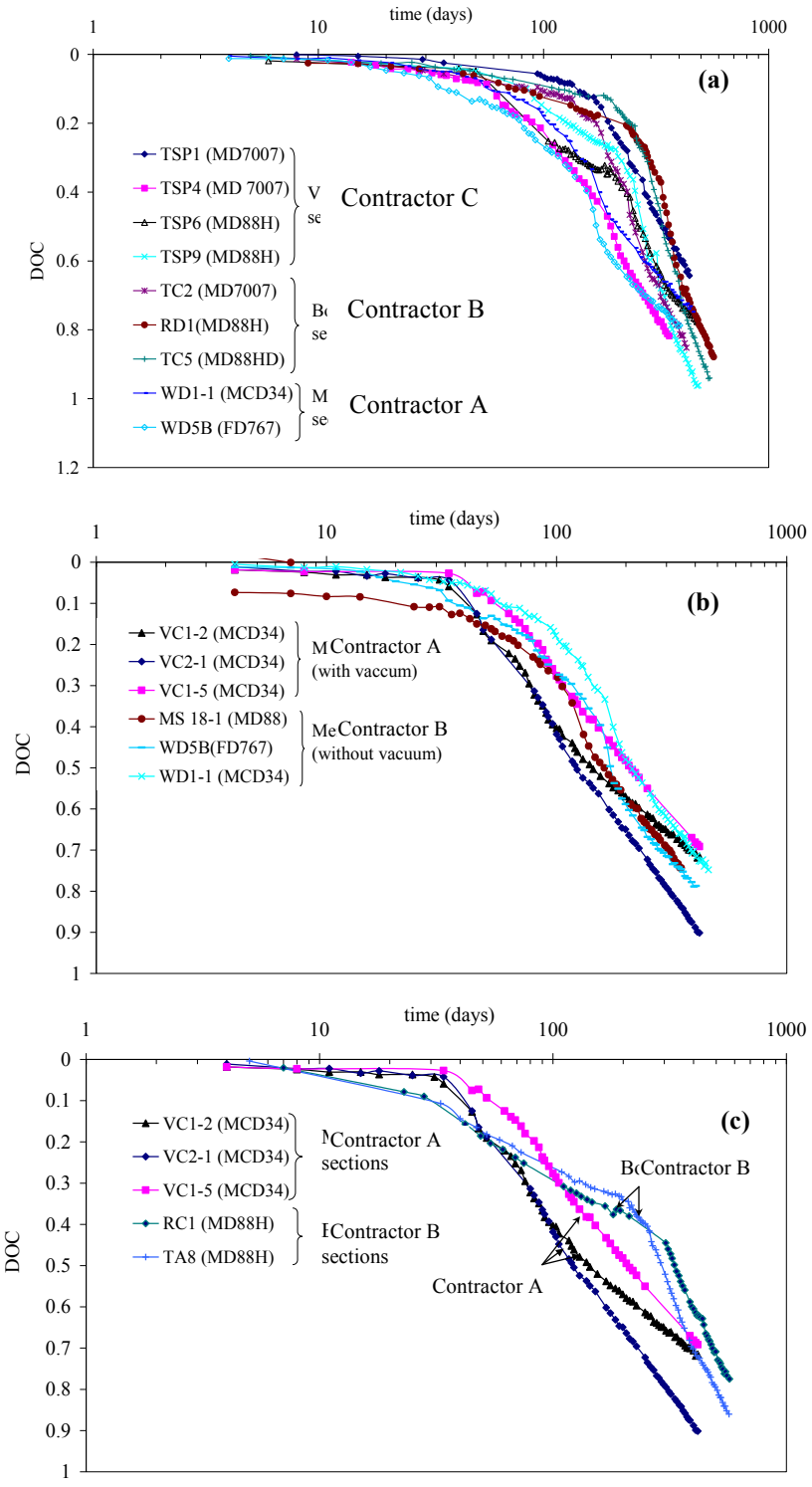

Figure 6: Analytically computed DOC with time for (a) non-vacuum in S3A and T11, (b) treatment in S3A only and (c) vacuum areas in S3A and T11.

The *β-factor* is dimensionless parameter introduced to capture the drain and site loading conditions for a given depth of soil, and it is totally independent of the soil properties. It is a useful parameter that can distinguish the relative effectiveness between different methods of treatment apart from the conventional degree of consolidation, and reflects the favourable effects of: (i) increasing the drain length (l_d), (ii) decreasing the drain spacing (S_d) and its pattern (α =

1.05 for triangular and 1.13 for square spacing), and (iii) increasing the surcharge load height (H) to consolidate the given clay thickness (h_c), represented by the ratio (H/h_c).

In this respect, this dimensionless parameter β can be defined as:

$$\beta = (l_d/\alpha s_d) \times (H/h_c)$$

Based on the magnitude of β determined at each settlement plate location for S3A and T11, the drain and site conditions at the 3 trial paddocks can be differentiated as:

(i) Low β impact: 2-6 (for S3A area under Contractor A),

(ii) Moderate β impact: 8-12 (for T11 area under Contractor B) and

(iii) High β impact: 12 -18 (for T11 area under Contractor C).

Although the value of β has no specific relationship to the converging target of DOC intended to be attained at the date of fill removal by all contractors, it can act as a 'filter' in distinguishing the relative performance in S3A and T11, by dividing the DOC by β. Figure 7 shows the variation of DOC divided by β-factor (U/β) plotted against time. This results in a separation between vacuum and non-vacuum areas, and also separates the vacuum consolidation effects of Contractors A and B. When considering all 3 sets of plots (Figs. 7a-c), the relative consolidation performance seems more superior in the case of Contractor A treatment areas when using vacuum consolidation, in comparison with all other locations in S3A and T11.

4.2 EXCESS PORE WATER PRESSURE DISSIPATION

Figure 8 shows the reduction in pore water pressure with time and it is observed that VC2 in |S3A shows the largest reduction closely followed by VWP3 in T11 (Contactor C). However, because of the varying fill heights and clay thickness in S3A and T11 paddocks these plots cannot be directly compared and most of them are clustered together during the first 3 months showing little differences. Figure 9a indicates the rate of change of excess pore water pressure for the same locations, and it is observed that VC2, VC1 and WD1 indicate the highest rate of change of excess pore pressure at the start, with VC1 maintaining a steady state over a long period of time. The membraneless systems do not seem to indicate a high rate of excess pore pressure dissipation in comparison with VC1 and VC2 areas. When these plots are normalised by the β-factor (Figure 9b), it is clearer that VC1 and VC2 provide the best treatment in view of excess pore pressure dissipation, compared to all other areas. While the fill height is reduced in VC areas of S3A thereby involving less mucking operations, the applied suction (-70 kPa) more than compensates for accelerated excess pore pressure dissipation rates, confirming the effective performance of membrane-type vacuum consolidation technique.

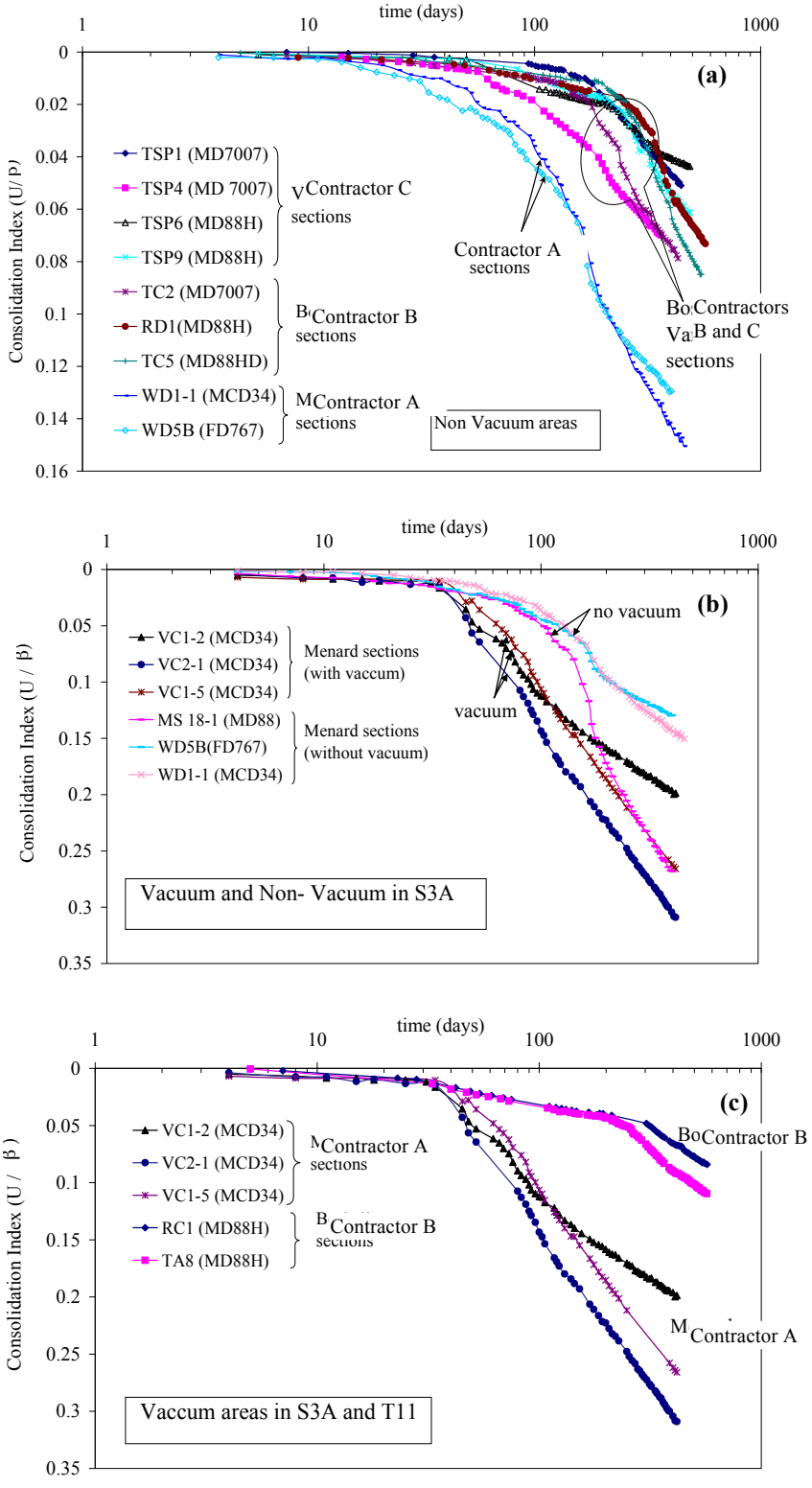

Figure 7: Computed DOC/β with time for (a) non-vacuum in S3A and T11, (b) treatment in S3A only and (c) vacuum areas in S3A and T11.

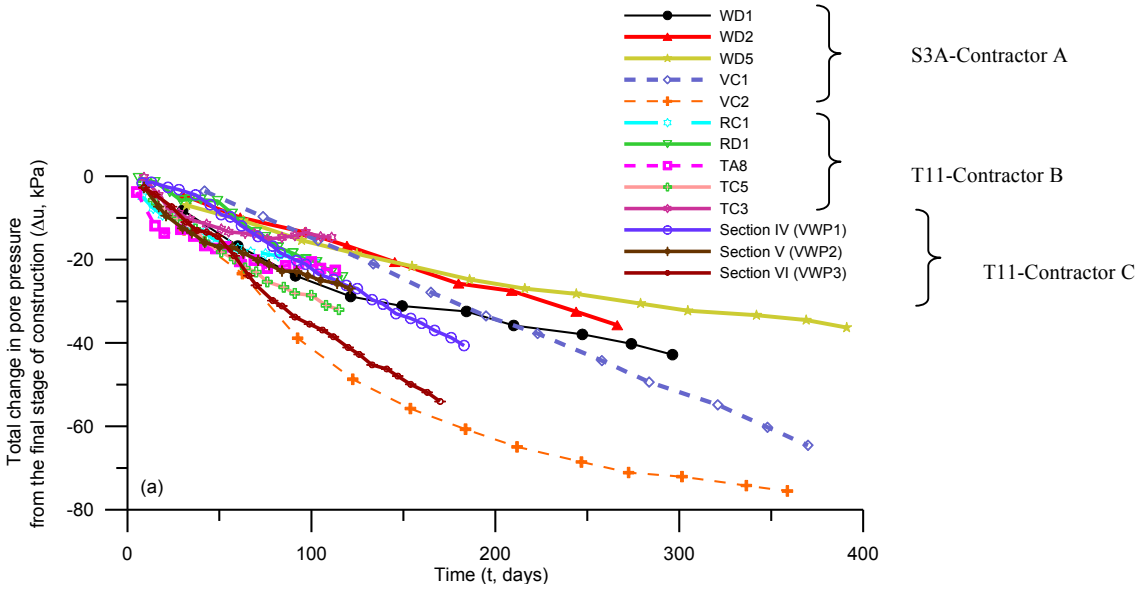

Figure 8: Reduction in Excess Pore Water Pressure with Time in S3A and T11 areas.

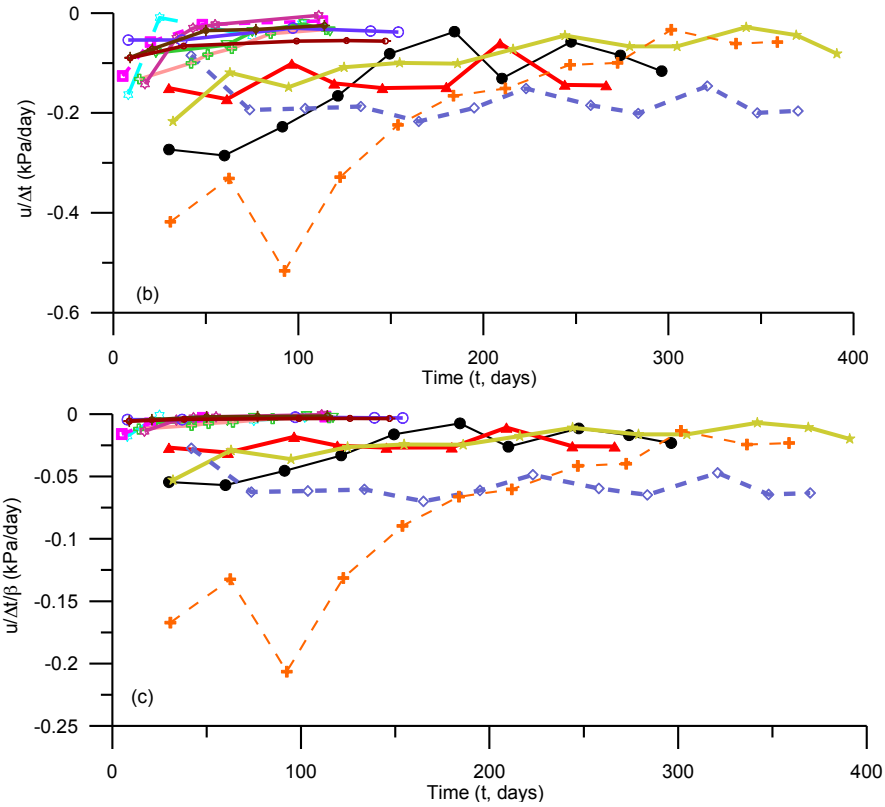

Figure 9: Comparison of excess pore pressure dissipation between S3A and T11 (a) Rate of dissipation of Excess pore pressure, (b) Excess pore pressure dissipation rate normalised by β.

4.3 CONTROLLING THE LATERAL DISPLACEMENTS

It is well-known that the vertical drains have the advantage of reducing the lateral yield in soil and that the application of vacuum pressure further controls the lateral movement, and in some cases may even make the lateral movements go inwards rather than outwards (Indraratna *et al.*, 1997, Indraratna *et al.*, 2005). The use of vacuum pressure to attain strict control of lateral displacements will be very important in sensitive areas such as in the vicinity of marine parks. In this particular POB site, only very limited field data has been available from a few inclinometers. Nevertheless, in order to compare the lateral movements of selected vacuum and non-vacuum areas that have very different soil profile and surcharge load conditions, the lateral displacement can be divided by the applied effective stress at the same depth.

The normalised lateral displacement profiles with depth for the limited data sections are shown in Figure 10. These four plots clearly indicate that while vacuum consolidation is definitely beneficial for controlling the lateral movement, the Menard vacuum system with 70 kPa suction further demonstrates the most significant reduction in the normalised lateral displacement (i.e. compare VC1-MS28 with WD3-MS27). In the Membraneless vacuum system with 50 kPa suction, while a reduction in the lateral movement is definitely achieved (i.e. compare MS24 with MS34), the amount of this reduction is not as significant as that of Membrane system. The shape of the lateral displacement curves suggest that in all VC areas the suction head propagates significantly with depth such that both the LHC and UHC layers are favourably influenced.

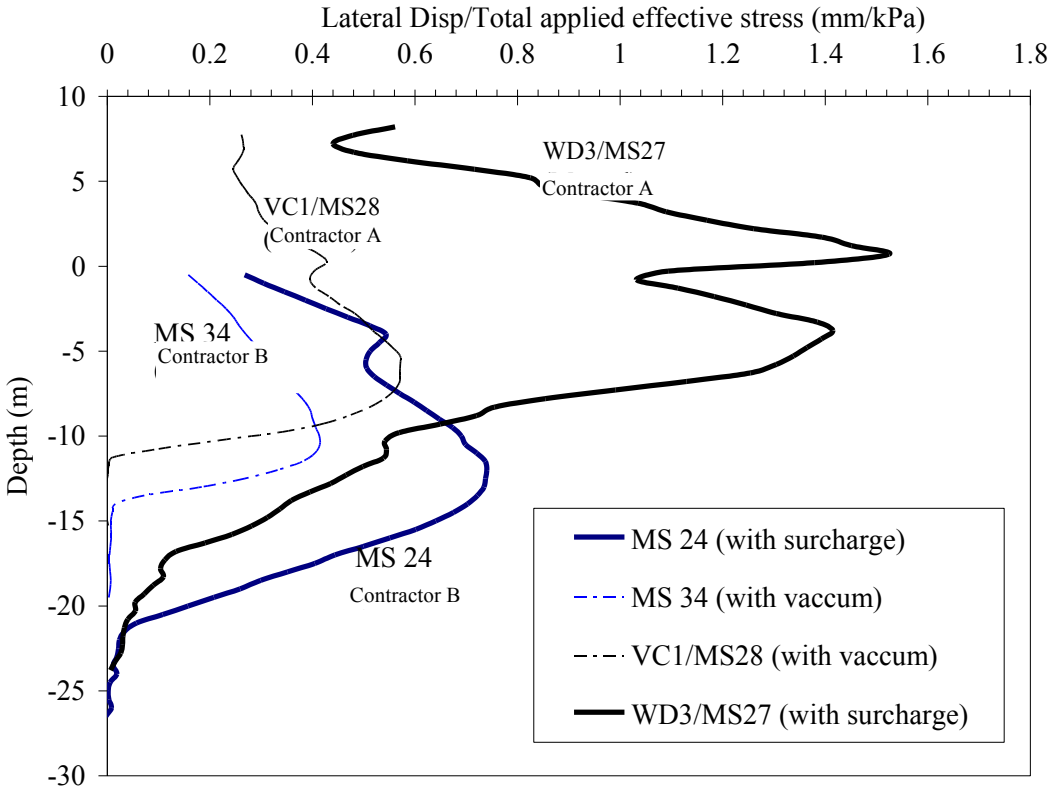

Figure 10: Role of Vacuum Consolidation on Lateral Displacement.

4.4 RESIDUAL SETTLEMENTS (RS)

All contractors have efficiently controlled the residual settlements, either to be less than 150 mm or 250 mm depending on the clay thickness and anticipated service loads in the respective areas. In Figure 11, the values of RS for both S3A and T11 paddocks are calculated plotted with the *β-factor* based on methods provided by Terzaghi *et al*., (1996); Yin and Graham, (1994) and the observations suggest that the critical RS occurs in the range $4 < \beta < 16$. In this critical zone, that includes locations from all 3 contractors from both S3A and T11 paddocks, the RS are close to the permissible limits. At low values of $\beta < 4$, the residual settlements are much smaller mainly because of vacuum consolidation. At very high values of $\beta > 16$ (T11), the RS tend to decrease mainly because of the high fill surcharge levels compared to the clay thickness (i.e. relatively high H/h_c ratio).

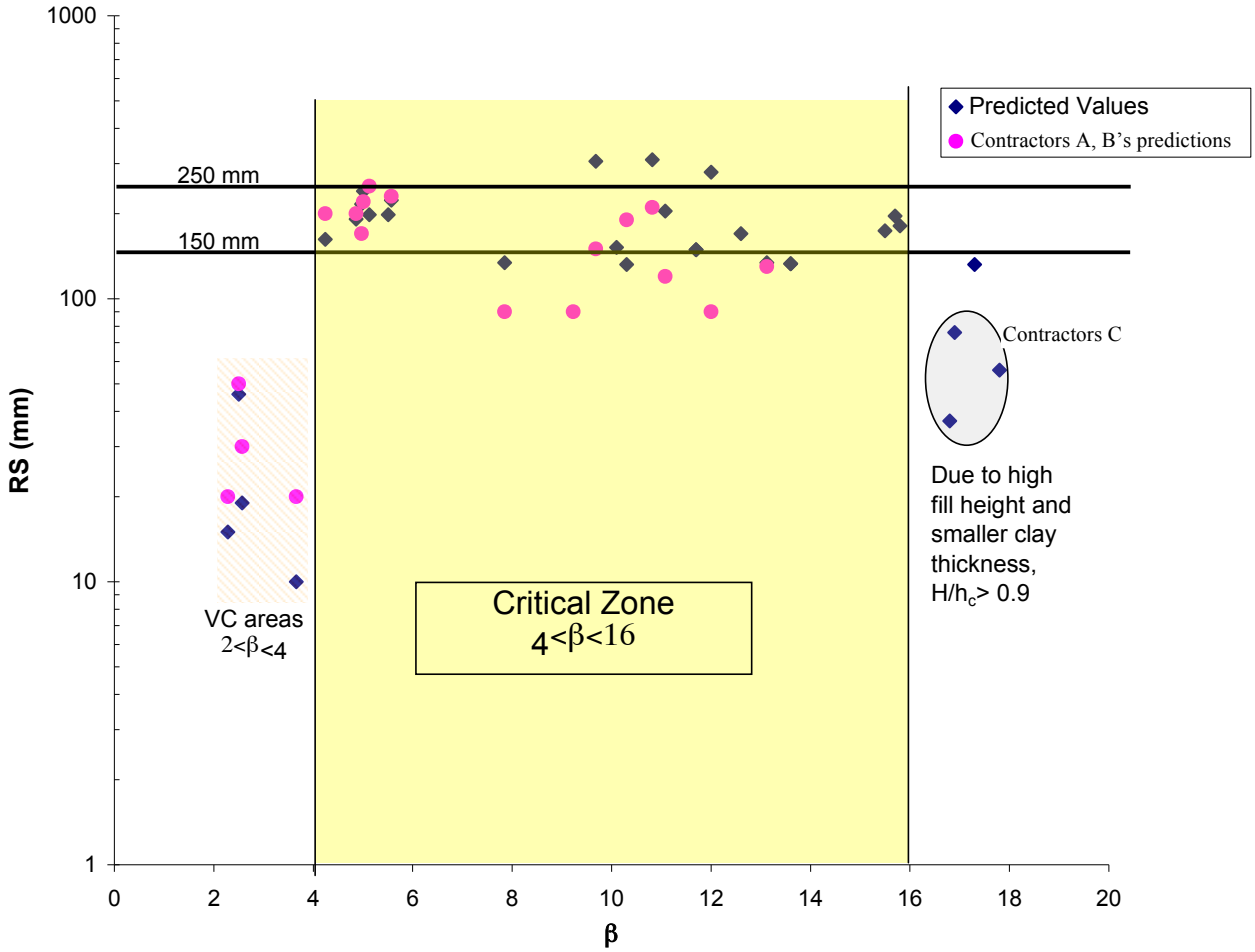

Figure 11: Critical β values for permissible Residual Settlement in S3A and T11.

Figure 12 provides approximately linear relationships between the RS and clay thickness for a range of OCR from 1.1 to 1.4 for DOC exceeding 80%. As expected, it is observed that when the OCR increases the RS decreases substantially. In general, as the total Holocene clay thickness increases, the RS also increases, and the corresponding regression lines and best–fit equations are also provided on Figure 12. In particular, the vacuum consolidation locations of S3A (VC1-2, VC2-2 and VC2-3) show considerably reduced RS at OCR approaching 1.4, well below the permissible limit. At an OCR of approximately 1.3, the residual settlements associated with membraneless consolidation (TA8,) and VC1-5 (S3A) are also small.

Based on Figure 12, a lower bound and upper bound for RS in terms of clay thickness (h_c) can be obtained as follows for the entire range of over-consolidation upon fill removal:

Lower Bound: RS = 3.8 h_c – 27 (vacuum consolidation in S3A at OCR = 1.4)

Upper Bound: RS = 14.3 h_c + 34 (surcharge only sites at OCR = 1.1)

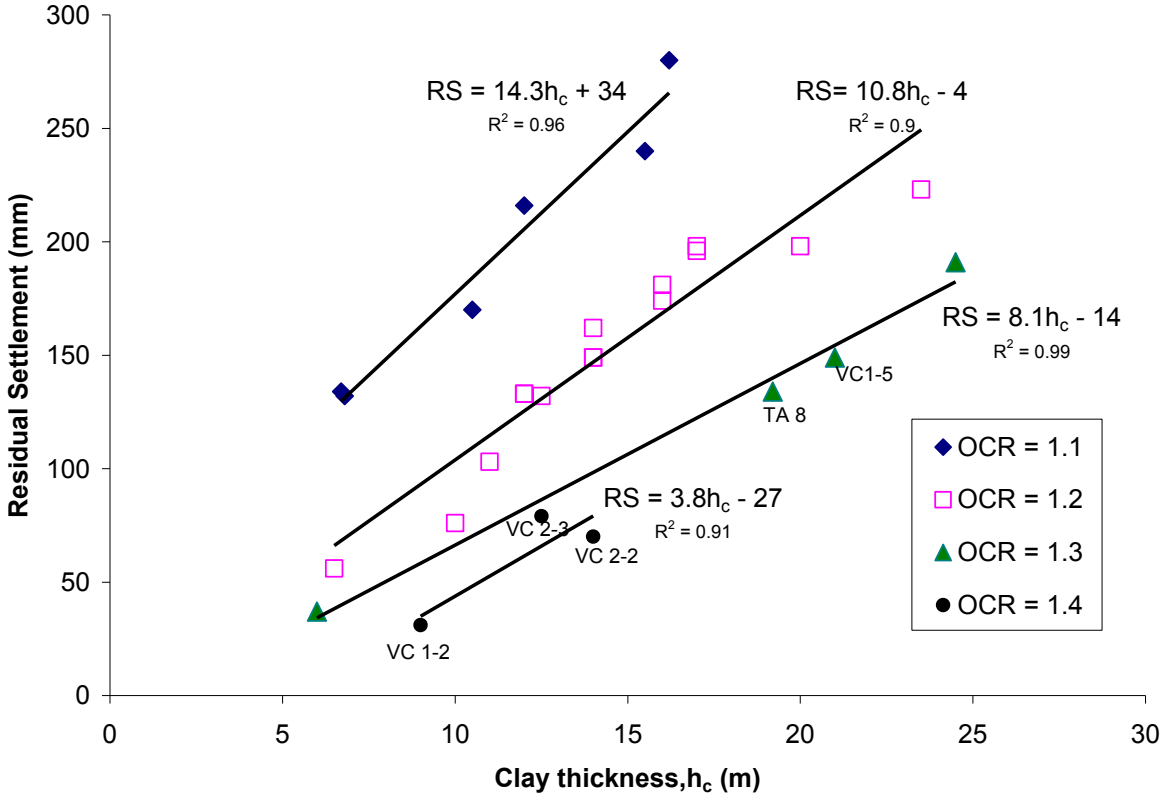

Figure 12: Effect of OCR and Clay Thickness on Residual Settlement

In order to predict excess pore pressures and associated settlements, Equations (11)-(21) are employed in conjunction with Tables 1 and 2 that summarise the soil properties for each layer and soil thickness for each section, respectively. In the analysis, the value of soil compression index (C_c) obtained from the oedometer test is related to the actual stress state within a given region of the foundation. The vertical and horizontal coefficients of consolidation were determined using the oedometer and Rowe cells. For the completely remoulded dredged mud that was reclaimed from the seabed and Upper Holocene Sand the ratio k_h/k_s were assumed to be unity. For the upper and lower Holocene clay, the ratios of k_h/k_s and d_s/d_w were assumed to be 2 and 3, respectively, in accordance with the laboratory tests conducted by Indraratna and Redana (2000); Indraratna *et al*. (2008); Ghandeharioon *et al.* (2010).

Table 1: Soil profiles, equivalent drain diameter and drain influence zone diameter used for prediction (Indraratna et al. 2011)

Area	Layer Thickness (m)				Drain influence zone diameter (m)	Equivalent drain diameter (m)
	Dredged mud	Upper Holocene sand	Upper Holocene Clay	Lower Holocene Clay		
WD1	2	1	4	11.5	1.23	0.034
WD2	2	1.5	2	19	1.57	0.034
WD3	2	1	2	8	1.24	0.05
WD4	2	1.5	2	21	1.47	0.05
WD5A	0	1	2	8	1.36	0.05
WD5B	2.5	1	2	7	1.24	0.05
VC1	2.5	2.5	2	5	1.36	0.034
VC2	0.5	3	2.5	16	1.36	0.034

Table 2: Soil properties for each layer (Indraratna *et al*., 2011).

Soil layer	Soil type	γ_t (kN/m^3)	Cc/(1+e$_0$)	c_v (m^2/yr)	c_h (m^2/yr)	k_h/k_s	$s=d_s/d_w$
1	Dredged Mud	14	0.235	1	1	1	1
2	Upper Holocene Sand	19	0.01	5	5	1	1
3	Upper Holocene Clay	16	0.18	1	2	2	3
4	Lower Holocene Clay	16	0.2	0.8	1.9	2	3

The embankment load was simulated according to a staged construction (with compacted unit weight of 20 kN/m^3). Settlement and associated excess pore pressure predictions were conducted at the embankment centreline using the proposed analytical model. As the computation of consolidation settlement and excess pore pressure at the centreline (zero lateral displacements) is straightforward and follows the basic 1-D consolidation theory, the use of a MATLAB spreadsheet formulation was most convenient. It is noted that, at the beginning of each subsequent stage, the initial *in situ* effective stress was calculated based on the final degree of consolidation of the previous stage. In vacuum areas, the suction pressure of 65 kPa was used to compute the settlement and excess pore pressure.

Figures 13 and 14 show the calculated settlements and associated excess pore pressures with the measured data in Areas WD4 and VC1. Overall, the comparisons between prediction and field observation show that the settlement and associated pore water pressure can be predicted very well. In vacuum areas, the degree of consolidation exceeded 90% at 400 days, whereas that in the non-vacuum area was less than 85% at the same time. This confirms that, at a given time, the vacuum combined preloading would accelerate consolidation faster than the surcharge preloading alone. This is because in non-vacuum areas, a gradual embankment construction had to be followed to avoid potential undrained failure in the remoulded dredged layer.

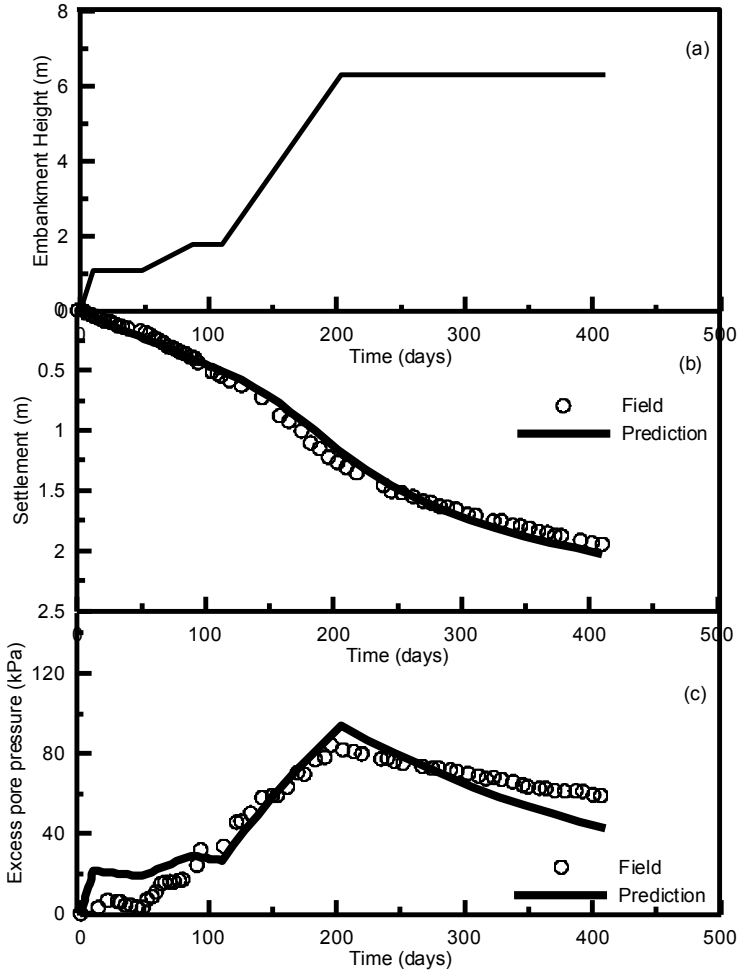

Figure 13: WD4 area: (a) stages of loading, (b) surface settlements under the embankment centreline and (c) excess pore pressures 4.

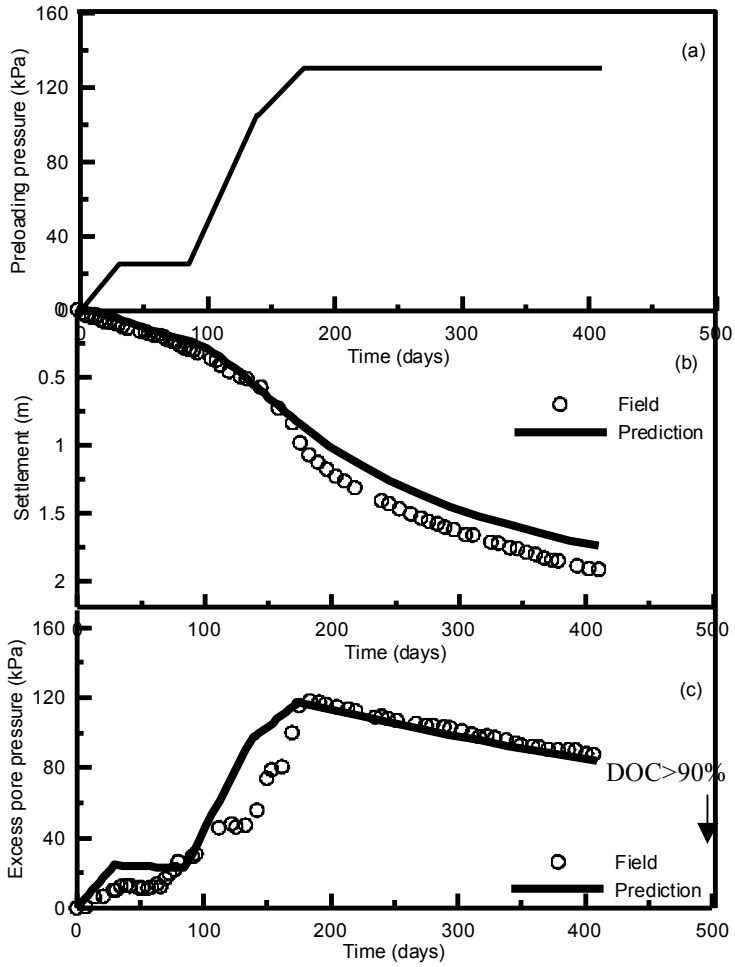

Figure 14: VC1 area: (a) stages of loading, (b) surface settlements under the embankment centreline and (c) excess pore pressures

5 CONCLUSIONS

A system of vertical drains with vacuum preloading is an effective method for speeding up soil consolidation. The performance of ground consolidation at the Port of Brisbane was analysed and discussed. The land was reclaimed using mud dredged from the seabed of shipping channels and berths. A total of 3 trial areas were chosen to study the behaviour of surcharge and vacuum consolidation. Purely on the basis of settlements of Degree of Consolidation (DOC), it is not possible to compare the relative treatments applied in the two paddocks S3A and T11. This is because, in all cases they achieved a relatively high target DOC irrespective of the type of drains and their installation pattern, nature of surcharge loading (with or without vacuum) and clay thickness. In order to magnify the differences between the trial locations, a drain and site representation factor totally independent of soil consolidation properties was defined as the *β-factor,* designed to capture the drain and site loading conditions. It comprises the favourable of effects of: (i) increasing the drain length (l_d), (ii) decreasing the drain spacing (S_d) and its pattern (α = 1.05 for triangular and 1.13 for square spacing), and (iii) increasing the surcharge load height (H) in relation to a given clay thickness (h_c).

Dividing the degree of consolidation, settlement and lateral displacement/settlement ratio by this β-factor, provides a performance indicator that represents the returns per unit value of β. In such a comparison, the vacuum consolidation applied by Contractor A in S3A seems to be the most beneficial. The membraneless vacuum system application is also effective in terms of controlling lateral displacement. However, the field inclinometer data is very limited to make overall conclusions. Control of lateral displacement effectively in sensitive areas such as marine parks would benefit immensely by the application of vacuum pressure and thereby decreasing the required fill heights on the surface.

While a distinct relationship between the DOC and RS is difficult to determine for the given conditions, there is no doubt that the RS decreases almost linearly with the increase in the over-consolidation ratio, and also the RS tends to become closer to the prescribed 150 mm limit for the critical range $4 < \beta < 16$. The minimum RS is attained in the vacuum consolidation sites in S3A when the OCR exceeds 1.3. The RS tends to become critical when the OCR is close

to or less than 1.1, and this situation mainly occurs for surcharge only sites with large clay thickness, where the treatment is not as effective as when vacuum pressure is applied. It verifies that a large surcharge fill height becomes necessary in the absence of vacuum pressure in order to keep the RS less than the prescribed limit, and the need to remove a large amount of fill in order to achieve a significant OCR can be a cumbersome process in the field. The higher the service load, the greater will be the advantage of vacuum application as a means of reducing the need for excessive fill heights as well as lateral displacement control. In view of stringent residual settlement and lateral displacement control plan, the application of sufficiently high vacuum pressure in tandem with some surcharge fill to achieve a relatively high DOC (i.e. > 85%) and subsequent unloading for attaining an OCR > 1.3 would be the optimum choice for the site characteristics and loading conditions encountered here.

The unit cell theory considering time-dependent surcharge load and vacuum application was developed to predict the settlement and the associated excess pore pressure, which were shown to be in good agreement with the field measurements. At 400 days, the degree of consolidation in the vacuum areas is much greater than the non-vacuum areas for the same total stress applied at the surface. The system of PVDs subjected to vacuum combined surcharge preloading is a useful method for accelerating the radial consolidation and for controlling the lateral displacement. While the analytical model discussed here is a useful tool to predict the performance of soft clay stabilized by PVDs, the accurate modelling of pressure preloading requires field observation to examine the correct vacuum pressure distribution, as the fluctuation of suction with time and with depth has not been uncommon in numerous case studies.

6 ACKNOWLEDGEMENTS

Writers acknowledge the support of the Port of Brisbane Corporation, Coffey Geotechnics and Austress Menard. The research funding from the Australia Research Council and Australia, Centre of Excellence for Geotechnical Science and Engineering is acknowledged. The assistance of Prof. A.S. Balasubramaniam of Griffith University, Daniel Berthier of Austress Menard Bachy, Prof Harry Poulos, Cynthia De Bok, Tine Birkemose and Chamari Bamunawita of Coffey Geotechnics is appreciated. More elaborate details of the contents discussed in the paper can also be found in previous publications of the first Author and his research students in ASCE and Canadian Geotechnical Journals, since the mid 1990's. Valuable comments from A/Prof Hadi Khabbaz of UTS are greatly appreciated.

7 REFERENCES

Ameratunga, J., Boyle, P., De Bok, C. and Bamunawita, C. (2010). Port of Brisbane (PoB) Clay Characteristics and Use of Wick Drains to Improve Deep Soft Clay Deposits. Proceedings 17th Asian Geotechnical Conference, Taipei, Vol I, pp 116-119.

Austress Menard (2008). Personal communication internal report and confidential, 79p.

Berthier, D., Boyle, P., Ameratunga, J., De Bok, C. and Vincent, P. (2009). A successful trial of vacuum consolidation at in the Port of Brisbane. PIANC 2009, Christchurch, New Zealand (in CD).

Chai, J.C., Carter, J.P., and Hayashi, S. (2005). Ground deformation induced by vacuum consolidation. Journal of Geotechnical and Geoenvironmental Engineering, 131(12):1552-1561.

Chu, J. Yan, S.W., and Yang, H. 2000. Soil improvement by the vacuum preloading method for an oil storage station. Geotechnique, 50(6): 625-632.

Geng, X. Y., Indraratna, B. and Rujikiatkamjorn, C. (2012). Analytical solutions for a single vertical drain with vacuum and time-dependent surcharge preloading in membrane and membraneless systems. International Journal of Geomechanics, ASCE, 12(1), 27-42.

Ghandeharioon, A., Indraratna, B., and Rujikiatkamjorn, C. (2010). Analysis of soil disturbance associated with mandrel-driven prefabricated vertical drains using an elliptical cavity expansion theory. International Journal of Geomechanics, ASCE. 10(2), 53-64.

Holtz, R. D., Jamiolkowski, M., Lancellotta, R. and Pedroni, S. (1991). Prefabricated vertical drains: design and performance. CIRIA ground engineering report: ground improvement. Butterworth-Heinemann Ltd, UK, 131.

Indraratna, B. and Redana, I. W. (2000). Numerical modeling of vertical drains with smear and well resistance installed in soft clay. Canadian Geotechnical Journal, 37: 132-145.

Indraratna, B., Balasubramaniam, A.S. and Sivaneswaran (1997). Analysis of Settlements and Lateral Deformation of Soft Clay Foundation beneath Two Embankments. International Journal of Numerical and Analytical Methods in Geomechanics, 31(9): 599-618.

Indraratna, B., Sathananthan, I., Rujikiatkamjorn C. and Balasubramaniam, A. S. (2005). Analytical and numerical modelling of soft soil stabilized by PVD incorporating vacuum preloading. International Journal of Geomechanics, 5(2). 114-124.

Indraratna, B., Aljorany, A., and Rujikiatkamjorn C., (2008). Analytical and Numerical Modelling of Consolidation by Sand Drains beneath a Circular Embankment. International Journal of Geomechanics, ASCE. 8(3), 199-206.

Indraratna, B., Rujikiatkamjorn, C., Ameratunga, J., and Boyle, P. (2011) Performance and Prediction of Vacuum Combined Surcharge Consolidation at Port of Brisbane. J. of Geotechnical & Geoenvironmental Engineering, ASCE, 137 (11), 1009-1018.

Mohamedelhassan, E., and Shang, J.Q. (2002). Vacuum and surcharge combined one-dimensional consolidation of clay soils. Can. Geotech. J. 39: 1126-1138.

Port of Brisbane Corporation (2009). Annual report 2008/2009, Port of Brisbane Corporation, Brisbane, Queensland, 92p.

Rujikiatkamjorn, C., Indraratna, B. and Chu, J. 2008. 2D and 3D numerical modeling of combined surcharge and vacuum preloading with vertical drains. International Journal of Geomechanics, 8(2): 144-156.

Sathananthan, I., Indraratna, B., and Rujikiatkamjorn C., (2008). The evaluation of smear zone extent surrounding mandrel driven vertical drains using the cavity expansion theory. International Journal of Geomechanics, ASCE. 8(6), 355-365.

Shang, J.Q., Tang, M., and Miao, Z. (1998). Vacuum preloading consolidation of reclaimed land: a case study. Canadian Geotechnical Journal, 35: 740-749.

Terzaghi, K., Peck, R. B. and Mesri, G., (1996) Soil Mechanics in Engineering Practice, 3rd Ed. Wiley-Interscience.

Yan, S.W. and Chu, J. (2003). Soil improvement for a road using a vacuum preloading method. Ground Improvement, 7(4): 165-172.

Yin, J.-H., and Graham, J. (1994). Equivalent times and one-dimensional elastic visco-plastic modelling of time-dependent stress-strain behaviour of clays. Canadian Geotechnical Journal, 31: 42-52.

APPENDIX A: ANALYTICAL SOLUTIONS

A1 MEMBRANE SYSTEM

The pore water pressure within the vertical drain and the average pore water pressure for membrane system, which can be solved by considering the applicable boundary conditions and loading pattern (detailed derivations can be found in Appendix A), in the Laplace frequency domain are:

$$\hat{u}_{w1}(Z,S) = X_1 e^{a_1 Z} + X_2 e^{-a_1 Z} + X_3 e^{a_2 Z} + X_4 e^{-a_2 Z} + \hat{Q}(S) \tag{11}$$

$$\hat{u}_{w2}(Z,S) = Y_1 e^{b_1 Z} + Y_2 e^{-b_1 Z} + Y_3 e^{b_2 Z} + Y_4 e^{-b_2 Z} + \hat{Q}(S) \tag{12}$$

$$\hat{\bar{u}}_1(Z,S) = X_1(1-\frac{a_1^2}{B_2})e^{a_1 Z} + X_2(1-\frac{a_1^2}{B_2})e^{-a_1 Z} + X_3(1-\frac{a_2^2}{B_2})e^{a_2 Z} + X_4(1-\frac{a_2^2}{B_2})e^{-a_2 Z} + \hat{Q}(S) \tag{13}$$

$$\hat{\bar{u}}_2(Z,S) = Y_1(1-\frac{b_1^2}{B_4})e^{b_1 Z} + Y_2(1-\frac{b_1^2}{B_4})e^{-b_1 Z} + Y_3(1-\frac{b_2^2}{B_4})e^{b_2 Z} + Y_4(1-\frac{b_2^2}{B_4})e^{-b_2 Z} + \hat{Q}(S) \tag{14}$$

where,

$$a_1 = \sqrt{\frac{(\frac{\Theta}{C}+B_1+B_2)+\sqrt{(\frac{\Theta}{C}+B_1+B_2)^2-4\frac{\Theta}{C}B_2}}{2}}$$

$$a_2 = \sqrt{\frac{(\frac{\Theta}{C}+B_1+B_2)-\sqrt{(\frac{\Theta}{C}+B_1+B_2)^2-4\frac{\Theta}{C}B_2}}{2}}$$

$$b_1 = \sqrt{\frac{(\Theta+B_3+B_4)+\sqrt{(\Theta+B_3+B_4)^2-4\Theta B_4}}{2}}$$

$$b_2 = \sqrt{\frac{(\Theta+B_3+B_4)-\sqrt{(\Theta+B_3+B_4)^2-4\Theta B_4}}{2}}$$

$$\Theta = \frac{SK_3h_2^2}{n^2}$$

By considering the boundary conditions (Equations10a-10f), the continuity conditions at the interface between the underlying soil and sand blanket (Equations 10g-10j), and the initial condition (Equation 10k), the following matrix can be obtained to get X_i and Y_i ($i = 1,2,3,4$):

$$\xi_{8\times8}\psi^T = P^T \tag{15}$$

where $\xi_{8\times8}$ as Appendix A shows,

$$\boldsymbol{\psi} = \begin{bmatrix} X_1 & X_2 & X_3 & X_4 & Y_1 & Y_2 & Y_3 & Y_4 \end{bmatrix},\ \mathbf{P} = \begin{bmatrix} \hat{P}-\hat{Q}, & 0, & 0, & 0, & 0, & 0, & 0, & 0 \end{bmatrix}$$

$$B_1 = \frac{8K_1h_2^2}{F_{a1}n^2}, \qquad B_2 = \frac{8h_2^2\left(n^2-1\right)K_2}{F_{a1}n^2}, \qquad B_3 = \frac{8K_3h_2^2}{F_{a2}n^2}, \qquad B_4 = \frac{8h_2^2\left(n^2-1\right)K_4}{F_{a2}n^2},$$

$$F_{a1} = (\ln n - \frac{3}{4})\frac{n^2}{n^2-1} + \frac{1}{n^2-1}(1-\frac{1}{4n^2}),$$

$$F_{a2} = (\ln\frac{n}{m} + K_5\ln m - \frac{3}{4})\frac{n^2}{n^2-1} + \frac{m^2}{n^2-1}(1-K_5)(1-\frac{m^2}{4n^2}) + K_5\frac{1}{n^2-1}(1-\frac{1}{4n^2}),$$

$n=\frac{r_e}{r_w}$, $m=\frac{r_s}{r_w}$, $s=r_s/r_w$, $c_{vi}=\frac{k_{vi}}{m_{vi}\gamma_w}$, $c_{hi}=\frac{k_{hi}}{m_{vi}\gamma_w}$, $K_1=\frac{k_{h1}}{k_{v1}}$, $K_2=\frac{k_{h1}}{k_w}$, $K_3=\frac{k_{h2}}{k_{v2}}$, $K_4=\frac{k_{h2}}{k_w}$, $K_5=\frac{k_{h2}}{k_{s2}}$, $h_2=\frac{H}{d_w}$, $T_{h2}=\frac{c_{h2}\cdot t}{de^2}$, $C=\frac{c_{v1}}{c_{v2}}$, $Z=\frac{z}{H}$.

And $\hat{u}_{w1}(Z,S)$, $\hat{u}_{w2}(Z,S)$, $\hat{\bar{u}}_1(Z,S)$, $\hat{\bar{u}}_2(Z,S)$, $\hat{Q}(S)$, S is the Laplace transform of $u_{w1}(Z,T_{h2})$, $u_{w2}(Z,T_{h2})$, $\bar{u}_1(Z,T_{v1})$, $\bar{u}_2(Z,T_{v1})$, $q(T_{h1})$, T_{h2}.

The solutions to the excess pore water pressure u_{wi} and average pore water pressure $\bar{u}_i$ $(i=1,2)$ were obtained using the inverse Laplace transform of Equationss. (11) - (14), hence:

$$u_{wi}(Z,S)=\frac{1}{2\pi I}\int_{a-I\infty}^{a+I\infty}\hat{u}_{wi}(Z,S)e^{ST}dS \quad (i=1,2) \tag{16}$$

$$\bar{u}_i(Z,S)=\frac{1}{2\pi I}\int_{a-I\infty}^{a+I\infty}\hat{\bar{u}}_i(Z,S)e^{ST}dS \quad (i=1,2) \tag{17}$$

where, $I=\sqrt{-1}$. The analytical solutions of Equations (16) and (17) were obtained using the numerical inversion of Laplace transform.

A2 MEMBRANELESS SYSTEM

Similar as the membrane system, the pore water pressure within the vertical drain and the average pore water pressure for membraneless system, which can be solved by considering the applicable boundary conditions and loading pattern (Appendix A), in the Laplace frequency domain are:

$$\hat{u}_w(Z,S)=\chi_1e^{b_1Z}+\chi_2e^{-b_1Z}+\chi_3e^{b_2Z}+\chi_4e^{-b_2Z}+\hat{Q}(S) \tag{18}$$

$$\hat{\bar{u}}(Z,S)=\chi_1(1-\frac{b_1^2}{B_6})e^{b_1Z}+\chi_2(1-\frac{b_1^2}{B_6})e^{-b_1Z}+\chi_3(1-\frac{b_2^2}{B_6})e^{b_2Z}+\chi_4(1-\frac{b_2^2}{B_6})e^{-b_2Z}+\hat{Q}(S) \tag{19}$$

The matrix from the Equations (18) and (19) are determined by:

$$\xi'_{4\times4}\psi'^{T}=P'^{T} \tag{20}$$

where

ξ' as Appendix A shows,

$$\boldsymbol{\psi}'=\left[\chi_1 \quad \chi_2 \quad \chi_3 \quad \chi_4\right],\ \mathbf{P}'=\left[\hat{P}-\hat{Q},\ 0,\ (\eta-1)\hat{P},\ 0\right]$$

$$F_a=(\ln\frac{n}{m}+K_5\ln m-\frac{3}{4})\frac{n^2}{n^2-1}+\frac{m^2}{n^2-1}(1-K_5)(1-\frac{m^2}{4n^2})+K_5\frac{1}{n^2-1}(1-\frac{1}{4n^2})$$

$$B_5=\frac{8K_3h_2^2}{n^2F_a},\ B_6=\frac{8h_2^2\left(n^2-1\right)K_4}{F_{a2}n^2}.$$

Using the inverse Laplace transform, the excess pore water pressure u_w and average pore water pressure $\bar{u}$ can be obtained.

The settlement of the soil is given by:

$$s\left(t\right)=\int_{L_w}^{H}\varepsilon_2dz \tag{21}$$

Theoretically, the average degree of consolidation may be defined either in terms of strain or pore pressure. While the former shows the rate of settlement, the latter indicates the dissipation rate of excess pore water pressure.

The average degree of consolidation in terms of settlement can be expressed as:

$$\bar{U}_s=1-\frac{m_{v1}\int_0^{\rho}L^{-1}\left(\hat{\bar{u}}_1\right)dZ+m_{v2}\int_{\rho}^{1}L^{-1}\left(\hat{\bar{u}}_2\right)dZ}{m_{v1}\int_0^{\rho}(q_u-p)dZ+m_{v1}\int_{\rho}^{1}(q_u-p)dZ} \tag{22}$$

The average degree of consolidation may be defined in terms of effective stress (i.e. dissipation of excess pore water pressure) as:

$$\bar{U}_p = 1 - \frac{\int_0^{\rho} L^{-1}\left(\hat{\bar{u}}_1\right)dZ + \int_{\rho}^{1} L^{-1}\left(\hat{\bar{u}}_2\right)dZ}{\int_0^{\rho}(q_u - p)dZ + \int_{\rho}^{1}(q_u - p)dZ} \tag{23}$$